Designing and Refining Ni(II)diimine Catalysts Toward the Controlled Synthesis of Electron-Deficient Conjugated Polymers

5 AUTHORS, INCLUDING:

Colin Bridges
University of Toronto
11 PUBLICATIONS **110** CITATIONS

SEE PROFILE

Theresa M Mccormick
Portland State University
27 PUBLICATIONS **1,190** CITATIONS

SEE PROFILE

Dwight Seferos
University of Toronto
88 PUBLICATIONS **3,708** CITATIONS

SEE PROFILE

Designing and Refining Ni(II)diimine Catalysts Toward the Controlled Synthesis of Electron-Deficient Conjugated Polymers

Colin R. Bridges,[†] Theresa M. McCormick,[†] Gregory L. Gibson,[†] Jon Hollinger,[†] and Dwight S. Seferos*,[†,‡]

[†]Department of Chemistry, Lash Miller Chemical Laboratories, University of Toronto, 80 St. George Street, Toronto, Ontario M5S 3H6, Canada

[‡]Department of Chemical Engineering & Applied Chemistry, University of Toronto, 200 College Street, Toronto, Ontario M5S 3E5, Canada

Ⓢ *Supporting Information*

ABSTRACT: Electron-deficient π-conjugated polymers are important for organic electronics, yet the ability to polymerize electron-deficient monomers in a controlled manner is challenging. Here we show that Ni(II)diimine catalysts are well suited for the controlled polymerization of electron-deficient heterocycles. The relative stability of the calculated catalyst–monomer (or catalyst-chain end) complex directly influences the polymerization. When the complex is predicted to be most stable (139.2 kJ/mol), these catalysts display rapid reaction kinetics, leading to relatively low polydispersities ($\sim$1.5), chain lengths that are controlled by monomer:catalyst ratio, controlled monomer consumption up to 60% conversion, linear chain length growth up to 40% conversion, and 'living' chain ends that can be readily extended by adding more monomer. These are desirable features that highlight the importance of catalyst design for the synthesis of new conjugated polymers.
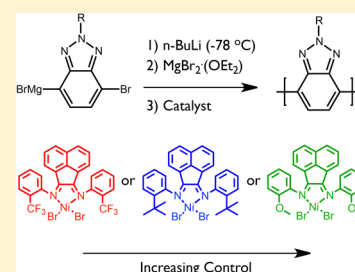
INTRODUCTION

Synthetic methodologies have continually benefitted from the design and development of catalysts, displaying greater activity, control, and functional group tolerance.[1−4] In conjugated polymer synthesis, the catalyst and monomer choice greatly affects the degree of control over molecular weight and polydispersity of the resulting polymer.[5−8] This is due to an association complex that forms between the catalyst and the growing polymer chain.[9−14] Weak association complexes lead to uncontrolled polymerization as is the case for nearly all electron-deficient monomers. Here we show that electron-donating Ni catalysts that associate more strongly with an electron-deficient monomer lead to increased control over the molecular weight and polydispersity. We found that by calculating the stabilization energy of the key association complex, density functional theory (DFT) calculations can accurately predict trends in catalyst effectiveness. Our most electron-rich catalyst exhibits controlled chain growth behavior with molecular weight control up to 25 kDa, chains that can be extended by adding more monomer, and a single type of end-group in the mass spectra. While still not as controlled as electron-rich polymers, we report M_n values that are as high as 32 kDa, with reasonably low polydispersity, making these polymers some of the best defined electron-deficient materials reported to date. These observations should motivate the improved design of other catalysts for the preparation of electron-deficient polymers and could allow for the controlled synthesis of well-defined n-type homopolymers or p−n block copolymers.

Current focus in π-conjugated polymer synthesis is mostly centered on polymer and hence monomer design. None-the-less, controlled methods to prepare π-conjugated polymers have matured greatly over the past 20 years. Efforts initially focused on controlling the regioregularity of poly-3-alkylthiophenes (P3AT) through selective monomer initiation or the use of selective nickel catalysts.[5−8] The subsequent discovery that under certain conditions 'living' polymerization character is observed led several researchers to study the mechanism of the controlled polymerization of alkylthiophenes. Nickel(II)-diphosphine catalysts are able to form a complex with the growing π-conjugated polymer chain and remain associated with the terminal repeat unit.[9−14] Small molecule competition experiments and computational studies provide further evidence that the controlled polymerizations of thiophenes are due to the catalyst forming a chain-associated nickel adduct.[15,16] From a materials perspective, these methodologies have been extended to selenophenes,[17] tellurophenes,[18] fluorenes,[19,20] and phenylenes[21,22] as well as the preparation of block-, gradient-, and statistical-type copolymers.[23−25] The ability to control molecular weight by the monomer:catalyst ratio has also made P3ATs a popular choice for structure−property-function studies.[26−31]

Ni(II)diphosphine catalysts, such as 1,2-bis-(diphenylphosphino)propane nickel(II) chloride and 1,2-bis-(diphenylphosphino)ethane nickel(II) chloride (Ni(dppe)Cl$_2$), are key enablers to the quasi-living polymerization of electron-

Scheme 1. Synthesis of 4,7-dibromo-2-(2-octyldodecyl)-2H-benzo[d][1,2,3]triazole (BTz)
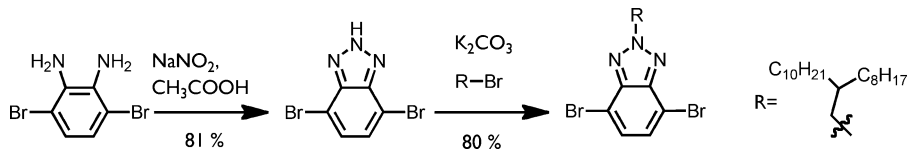
rich polyheterocycles, such as P3AT's. Palladium catalysts have been applied less frequently for the chain-growth polymerization of alternating electron-rich electron-poor π-conjugated units.[20,32] In contrast, catalysts applicable to the controlled chain growth polymerization of solely electron-deficient π-conjugated polymers have not yet been extensively developed.[33,38] Electron-deficient π-conjugated polymers with low-lying HOMO and LUMO levels are important as electron transport layers and also as air-stable organic electronic materials.[34−39] They are almost exclusively synthesized by polycondensation reactions possessing slow reaction kinetics exhibiting very little control over molecular weight and polydispersity. One clever example of the controlled polymerization of an electron-deficient moiety uses a naphthalenediimide derivative that forms a radical anion (the active monomer), thereby allowing for strong π-donation to the nickel catalyst.[40,41] While this method shows the characteristics of controlled chain growth, polymerization linkages were still made between electron-rich (thiophene) flanking groups. Moreover this mechanism is likely only applicable to monomers that form stable radical anions. It is currently thought that weakened π-donation to an electron-deficient conjugated system results in the poor control over polymerizations of electron-deficient monomers.[42−44]

■ RESULTS AND DISCUSSION

The chain-growth synthesis of conjugated polymers typically involves three steps: (1) preparing a dihaloheterocycle precursor; (2) generating an organometallic active monomer (typically a Grignard-type reagent); and (3) initiating polymerization with the catalyst (typically a nickel(II)diphosphine). Both the choice of catalyst and choice of monomer are important considerations. We therefore employed DFT calculations to predict the electronic structure of candidate electron-deficient polymers prior to synthesis. This lead us to select polybenzotriazole (PBTz) as our target polymer, since it is a polymer composed of electron-deficient units, and calculations on an eight-unit oligomer show electron-deficient character as noted by a predicted low-lying HOMO and LUMO levels relative to an eight-unit oligomer of P3AT (see the Supporting Information). The calculated electronic structure and experimentally determined HOMO and LUMO levels of this polymer are discussed later in the manuscript.

The dihalo precursor is prepared from 3,6-dibromobenzene-1,2-diamine (Scheme 1).[45] Treating 3,6-dibromobenzene-1,2-diamine with sodium nitrite and acetic acid affords 4,7-dibromo-2H-benzo[d][1,2,3]triazole in 81% yield.[46] Treating 4,7-dibromo-2H-benzo[d][1,2,3]triazole with potassium carbonate and 9-(bromomethyl)nonadecane affords 4,7-dibromo-2-(2-octyldodecyl)-2H-benzo[d][1,2,3]triazole (BTz) in 80% yield. The 2-octyldodecyl chain was chosen for this study after initial attempts using a less bulky side-chain (2-ethylhexyl) failed to produce soluble materials.

The selective preparation of the Grignard-type active monomer is important for controlled polymerizations to

proceed. Our initial attempts to form the active 4-bromo-7-chloromagnesio-2-(2-octyldodecyl)-2H-benzo[d][1,2,3]triazole monomer by treating BTz with isopropylmagnesium chloride lead to a significant amount of halogen exchange in both the 4 and 7 positions (determined by H⁺ quenching experiments, see the Supporting Information).[7] To improve the activation step, BTz was treated with n-butyllithium followed by magnesium bromide at −78 °C, a procedure adapted from the original McCullough synthesis of P3AT (Scheme 2).[5] The equilibrium

**Scheme 2. Typical Lithium−Halogen Exchange Metathesis and Polymerization Conditions**
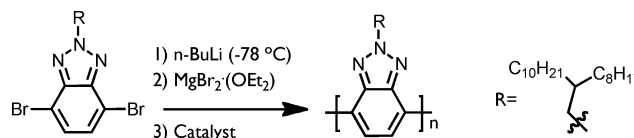
reached in the lithium−halogen exchange at cryogenic temperatures produces the mono exchanged species (verified by quenching experiments, see the Supporting Information). Subsequent treatment with the widely used Ni(dppe)Cl₂ catalyst affords the desired polymer, PBTz. Monitoring the molecular weight as a function of monomer consumption reveals limited chain growth behavior (see the Supporting Information), however polymerization took over 24 h, molecular weights were lower than expected based on monomer:catalyst ratio, polydispersity was high, and yields were 10% (Table 1).

Having determined that the widely used Ni(dppe)Cl₂ is not an ideal catalyst for this monomer, we now turn to the design of more suitable catalysts. We chose the Ni(II)diimine catalysts previously described by Brookhart and co-workers[47−49] that

Table 1. Molecular Weight and Polydispersity Data for Polymerization of (BTzC₂₀) Using the Three Catalysts

catalyst[a]	loading (mol %)	SEC M_n (kDa)[b]	expected M_n (kDa)[c]	PDI[b]	yield (%)
Ni(dppe)Cl₂	0.5	18.0	52	1.91	10
Ni(CF₃An)Br₂	2	13.5	13	2.36	25
	1	17.4	26	2.30	25
	0.5	23.7	52	2.16	50
Ni(t-BuAn)Br₂	2	13.5	13	2.12	29
	1	17.6	26	2.07	25
	0.5	19.1	52	2.10	43
Ni(OMeAn)Br₂	2	13.6	13	1.54	26
	1	24.3	26	1.66	57
	0.5	31.7	52	1.88	50

[a]Catalyst structures provided in Scheme 3. [b]M_n and PDI determined using SEC in 1,2,4-trichlorobenzene, 140 °C. [c]Expected M_n is estimated based on the measured M_n at 2% catalyst loading.

Scheme 3. Synthesis and Structure of Catalysts[a]
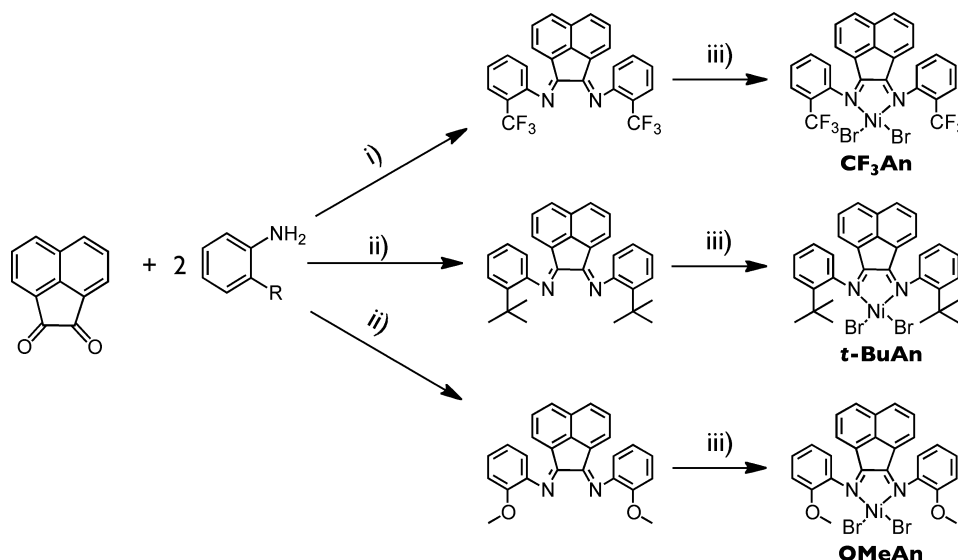
[a]Reagents and conditions: (i) R = CF_3, toluene (reflux), H_2SO_4 (cat.), 72 h; (ii) R = OMe or t-Bu, methanol (room temperature), formic acid (cat.), 16 h; (iii) nickel(II) bromide ethylene glycol dimethyl ether complex (Ni(DME)), dichloromethane.
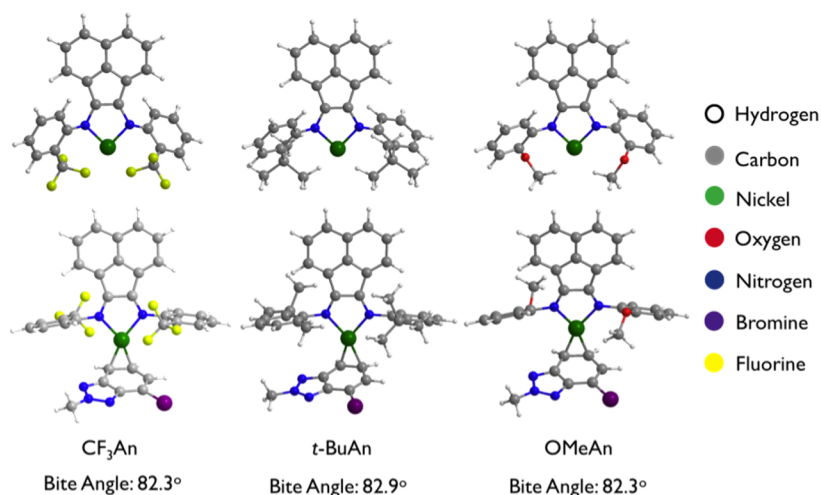

Figure 1. Optimized calculated geometries of the catalysts (top) and their association complex with the monomer (bottom).

have more recently been applied to aryl cross-coupling polymerizations due to their similar electron-donating ability to diphosphine ligands, and their ease of substitution in the 2 position. We chose acenaphthylene-(1,2-diylidene)bis(2-t-butylaniline) nickel(II) bromide (t-BuAn) as our parent catalyst since it is the only Ni(II)diimine that has been previously used for conjugated polymer synthesis.[50,51] Two other catalysts, each with different electron-donating/-withdrawing ability were then chosen from the parent: an electron-rich complex, acenaphthylene-(1,2-diylidene)bis(2-methoxyaniline nickel(II) bromide (OMeAn), and an electron-poor complex, acenaphthylene-(1,2-diylidene)bis(2-trifluoromethyl) nickel(II) bromide (CF_3An)[49] (Scheme 3). The optimized geometries of all three catalysts are predicted to have nearly the same bite angle (82.3–82.9 °), indicating that the accessibility of the Ni centers are all similar and our comparison to the more bulky t-butyl group would remain valid (Figure 1).

The critical step in the quasi-living chain growth mechanism is forming the π–Ni complex at the terminus of the growing chain, thus we first use DFT calculations to predict the strength

of this complex for each catalyst. Previous calculations on nickel catalysts and bromotoluene substrates conclude that the position of catalyst coordination on the asymmetric aromatic ring and the activation barrier to move to a new position on the ring are minimal.[53] Hence, we determine the association energy in the 3–4 position and compare it for our catalysts. To judge stability of the π–Ni complex, we calculate the total energy before and after catalyst association, then again after oxidative addition at the aryl bromide bond. Since both processes are exergonic, the dissociated monomer–catalyst pair is set to E = 0 kJ/mol, and the change in energy once the pair becomes associated is the strength of the π–Ni complex. The exergonic oxidative addition step in each case was also calculated to verify that it would be favorable for the catalytic cycle to proceed and that the π–Ni complex is not the most stable configuration.

Association energy with the electron-deficient monomer increases as a function of the electron-donating ability of the catalyst: from 59.1 to 101.5 to 139.2 kJ/mol for CF_3An, t-BuAn, and OMeAn, respectively (Figure 2). We anticipate that catalysts predicted to have stronger stabilization energies will
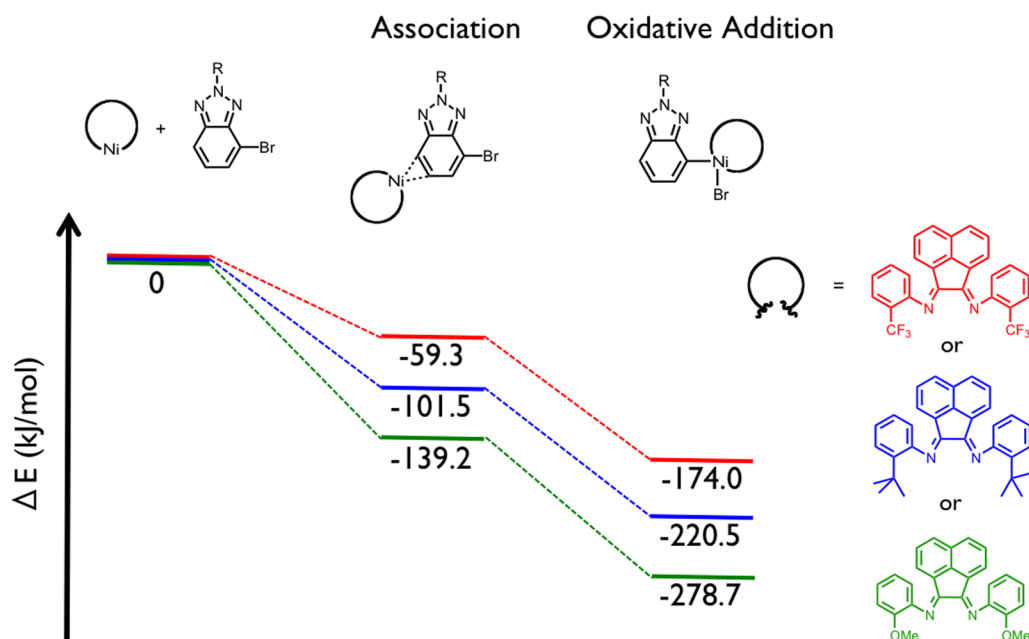
Figure 2. Reaction coordinate of the nickel catalysts associated with the monomer, followed by oxidative addition.

stay more effectively coordinated to the growing chain. This will reduce unwanted chain-coupling, termination, and reinitiation reactions and thus will exhibit more controlled polymerization with lower polydispersities and a chain-length that is better controlled by the monomer:catalyst ratio.

We synthesized each of the catalysts using methods adapted from those described by Brookhart and co-workers (Scheme 3). BTz was initiated using the optimized metathesis conditions and polymerized using each catalyst at three different monomer:catalyst ratios (0.5, 1, and 2 mol %). Following polymerization, the polymer was precipitated with methanol, washed with acetone, extracted with hexanes, and the molecular weight and polydispersity of the polymers was determined using size exclusion chromatography (SEC). Based on the observed higher molecular weights, higher yields, and much more rapid reaction kinetics (polymerizations were completed over the course of minutes rather than hours, see the Supporting Information), we can conclude that the Ni(II)-diimine catalysts are much more effective at polymerizing BTz than Ni(dppe)Cl$_2$.

One of the defining characteristics of controlled chain growth polymerizations is that since each catalyst initiates one chain, molecular weight can be controlled by the monomer:catalyst ratio. At 2 mol %, all three Ni(II)diimine catalysts produce M_n = 13–14 kDa polymers. For CF$_3$An and t-BuAn, molecular weight increases as catalyst loading decreases, however the increase is less than what would be expected for controlled chain growth polymerizations. For OMeAn, molecular weight increases by nearly an ideal factor of 2 (from 13.3 to 24.3 kDa) when the catalyst loading is reduced by a factor of 2. Molecular weight increases to 31.7 kDa when the catalyst loading is further decreased to 0.5% (Table 1), a value similar to what is observed for the living polymerization of thiophenes using the same catalyst loadings.[9] Compared to the electron-poor catalysts, OMeAn displays superior control over moleuclar weight, showing a linear dependence of molecular weight on monomer:catalyst ratio up to M_n = 24.3 kDa (Figure 4).

Polydispersity is an indication of how effective the catalyst is at controlling chain termination or transfer reactions during a

polymerization. At 2% catalyst loading, CF$_3$An, t-BuAn, and OMeAn yield polymers with polydispersities equal to 2.36, 2.12, and 1.54, respectively. The same trend is observed at 0.5 and 2 mol % catalyst loadings (Table 1). As hypothesized, termination and transfer reactions that increase polydispersity occur more frequently when the catalyst is not as strongly coordinated to the growing polymer chain. Examining the SEC elution profile of these polymers can indicate which termination reactions are occurring. It should be noted that in all polymerizations that use t-BuAn, high molecular weight shoulders are observed in the SEC elution curve. This shoulder is more pronounced when CF$_3$An is used, consistent with a higher probability of catalyst disproportionation and chain coupling.[50] The SEC elution profile for polymers prepared using OMeAn catalyst have a unimodal distribution (Figure 3).
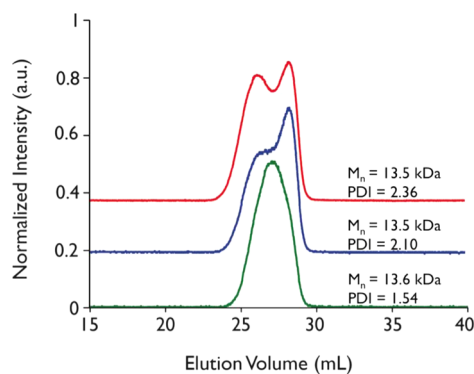

Figure 3. SEC elution profiles of PBTz at 2 mol % catalyst loading for CF$_3$An (red), t-BuAn (blue) and OMeAn (green).

In this case, the predicted catalyst coordination strength correlates well with how much control over the polymerization we can achieve with respect to molecular weight and polydispersity. This result highlights how DFT calculations can be accurately used to predict catalyst effectiveness and guide synthetic design.
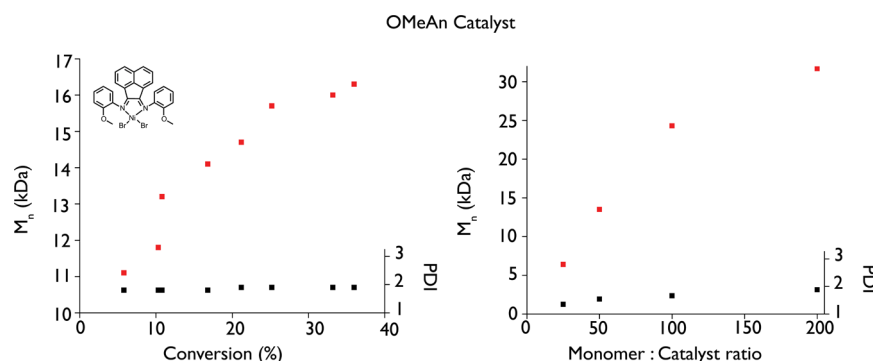
Figure 4. Molecular weight (red) and polydispersity (black) as a function of monomer conversion for PBTz at 1 mol % catalyst loading, 0.02 M monomer concentration (A). Molecular weight (red) and polydispersity (black) as a function of monomer:catalyst ratio for the OMeAn catalyst (B).
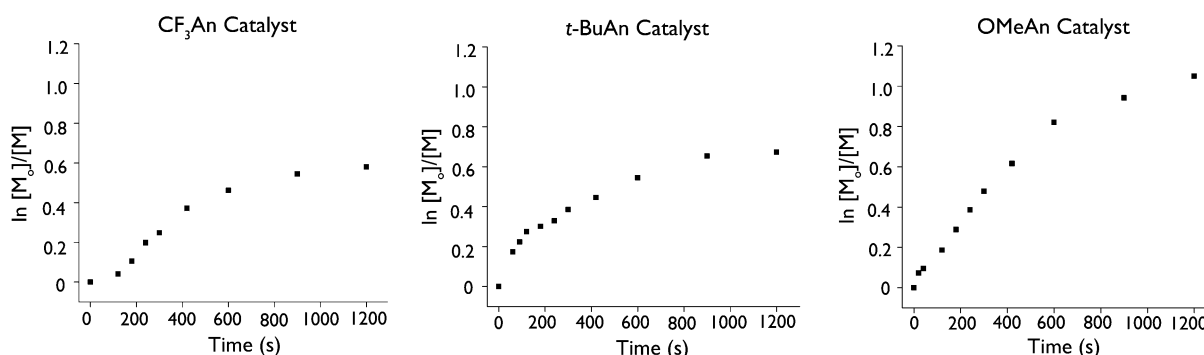

Figure 5. Semilogarithmic kinetic plots of BTz monomer consumption during polymerization at 0.5 mol % catalyst loading, 0.02 M monomer concentration.

Differences in initiation and propagation rates brought upon by the catalyst electronics can affect the measured polydispersity, however our results indicate the polydispersity is mainly broadened by increasing chain−chain coupling. Neither these coupling events, nor the control over molecular weight based on catalyst loading should be affected by initiation rates. As such we only discuss the molecular weight control and polydispersity with respect to the calculated coordination strength of the nickel catalyst.

Following the monomer consumption as a function of time can help compare the relative control each catalyst can achieve during a polymerization. These semilogarithmic kinetic plots are linear in the absence of termination reactions, thus deviations from linearity can indicate noncontrolled chain growth behavior. Comparing semilogarithmic plots for each catalyst reveals that the electron-rich catalyst, OMeAn, displays linearity up to 60% conversion, while the more electron-poor catalysts do not display a significant linear region (Figure 5). During polymerization using the OMeAn catalyst, polydispersities remain relatively low (around 1.7) until 60% conversion. These polymerizations exhibit quasi-living chain-growth kinetics with molecular weights depending linearly on conversion (Figure 4), which further indicates chain growth behavior. It should be noted that the propagation rate observed for Ni(II)diimine catalysts with BTz is similar to what is observed for Ni(dppe)Cl$_2$ with electron-rich monomers, such as thiophene.[9−11] Interestingly, previous studies using Ni(II)-diimine catalysts and thiophene monomers report only low molecular weight polymers.[51,52] For our polymerizations, monomer conversion plateaus at 40−50% for CF$_3$An and t-BuAn, and at ∼70% for OMeAn (see the Supporting Information). OMeAn is the superior catalyst, with respect to

yield, unimodal SEC trace, controlled molecular weight, and polydispersity (Table 1). While controlling the polymerization of electron-deficient polymers may not be possible to the extent that is observed for polythiophenes, using this catalyst M_n values greater than 30 kDa can be achieved, which are among the highest values reported for electron-deficient polymers.

The quasi-living nature of controlled chain growth polymerizations allows for extension of a polymer chain simply by adding more monomer once all the starting monomer has been consumed. We conducted a chain extension polymerization as follows: A flask with was charged with activated BTz monomer (0.30 mmol) and OMeAn catalyst to achieve a 4 mol % initial catalyst loading. The solution was allowed to polymerize for 15 min at room temperature, at which point the polymer molecular weight (M_n) was 6.4 kDa (PDI = 1.35). An additional aliquot of activated monomer (0.31 mmol) was added to achieve a 2 mol % catalyst loading. After an additional 15 min a polymer of nearly double the molecular weight results (M_n = 11.0 kDa; PDI of 1.52) (Figure 6). This chain extension behavior is unique to living and controlled polymerizations. Using MALDI-TOF mass spectrometry, we confirm that PBTz polymerized with OMeAn contains a single dominant set of end groups (H/Br terminated + 2K − H), consistent with controlled chain growth polymerizations (see the Supporting Information).

Cyclic voltammetry was conducted as a final experiment to confirm the electron-deficient nature of PBTz, (Figure 7). The polymer exhibits a quasi-reversible reduction with an onset −1300 mV relative to a ferrocene redox couple. The LUMO of PBTz lies at −3.5 eV, and the HOMO lies at −5.6 eV (based on the optical HOMO−LUMO gap ∼2.1 eV, see the Supporting Information). These values are significantly more
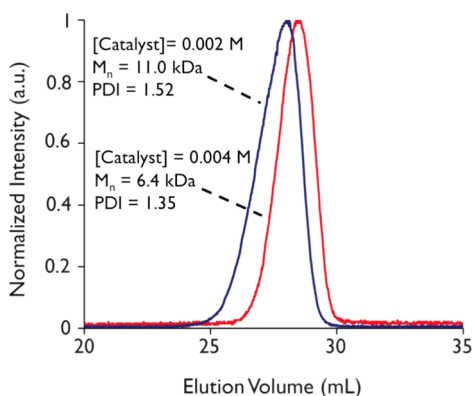
Figure 6. SEC elution profiles for the chain extension polymerization of BTz with 0.012 mmol OMeAn catalyst.
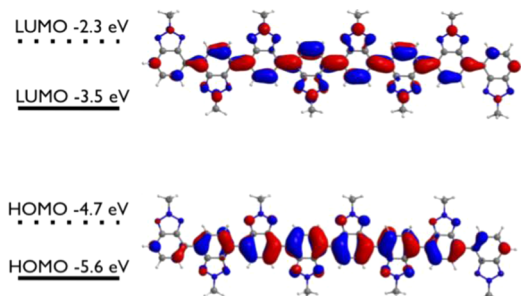

Figure 7. Cyclic voltammetry data (solid lines) and DFT calculations (dashed lines) of the HOMO and LUMO energies of polybenzotriazoles and eight-unit oligomers, respectively.

low-lying than polythiophenes and consistent with a polymer consisting of electron-deficient heterocycles. The optical band gap (2.1 eV) correlates well to the band gap calculated using DFT (2.4 eV). To probe possible electron-transfer from P3HT to PBTz, we also conducted fluorescence quenching experiments. In a 50:50 wt % PBTz:P3HT film, P3HT fluorescence is almost entirely quenched, indicating the lower lying LUMO of PBTz provides an alternative relaxation pathway for the excited state of P3HT (see the Supporting Information). Although not unexpected, this polymer exhibits electronic properties that are consistent with electron-deficient polymers.

CONCLUSIONS

We have designed, synthesized, and applied nickel(II)diimine catalysts for the controlled polymerization of an electron-deficient monomer and studied how catalyst electronics affects the computationally determined strength of the π−Ni complex. We found the strength of this association complex is a reasonably good predictor of control during polymerizations. As the calculated strength of the π−Ni complex increases, the polydispersity of the resulting polymer decreases, and the molecular weight becomes more controlled. To date, the controlled polymerization of electron-deficient polymers has been challenging. We have significantly improved the reaction kinetics and yield and most importantly gained control over polydispersity and molecular weight of an electron-deficient polymer relative to what is possible using typical catalysts. We feel that these points represent a significant advance in the controlled polymerization of electron-deficient conjugated materials and should motivate the improved design of other catalysts for the preparation of electron-deficient polymers.

Further, catalysts such as these could allow for the controlled synthesis of well-defined n-type materials.

EXPERIMENTAL SECTION

General Considerations. All reagents were used as received unless otherwise noted. Solvents THF and *N,N*-dimethylformamide were purchased from Caledon Laboratories Ltd., degassed, stored under nitrogen, and dried over molecular sieves prior to use. Methanol was purchased from EMD, hexanes and ethyl acetate were purchased from Caledon Laboratories Ltd. 1,2,4-trichlorobenzene (spectrophotometric grade), sulfuric acid (98%), and glacial acetic acid were purchased from Fisher Scientific. Formic acid (95%), sodium nitrite, potassium carbonate (anhydrous), acenapthenequinone, *o*-anisidine, nickel(II) bromide ethylene glycol dimethyl ether, magnesium bromide etherate (anhydrous), docosane (99%), and *n*-butyllithium (1.6 M in hexanes) were purchased from Sigma-Aldrich. 3,6-dibromobenzene-1,2-diamine was made from 2,1,3-benzothiadiazole (Sigma-Aldrich) using literature procedures.[45] 9-bromomethylnonadecane was prepared from 2-octyl-1-dodecanol using literature procedures.[68]

Instrumentation. Absorption spectra were recorded using a Varian Cary 5000 spectrometer. Fluorescence spectra were recorded using a PTI Quantamaster spectrofluorometer. Film absorption and fluorescence measurements were made using a glass substrate, polymer was spin coated from 10 mg/mL chloroform solution. NMR spectra were recorded on a Varian Mercury 400 spectrometer (400 MHz). Masses were determined on a Waters GCT Premier TOF mass spectrometer (EI). Polymer molecular weights were determined using a Viscotek HT-SEC module 350A (1,2,4-trichlorobenzene stabilized with butylated hydroxytoluene, 140 °C) with narrow weight distribution polystyrene standards using absorption at 486 nm. Electrochemistry was conducted using a BASi Epsilon EC potentiostat with polymer films drop cast onto a platinum button electrode from a 10 mg/mL solution in chloroform. Gas chromatography was conducted using a Perkin-Elmer Clarus gas chromatograph. MALDI spectra were obtained using a Waters MALDI micro MX TOF mass spectrometer from a 0.1 M dithranol matrix (10 000:1 matrix to polymer ratio) cast from chloroform.

Synthesis of 4,7-Dibromo-2H-benzo[*d*][1,2,3]triazole. 3,6-Dibromobenzene-1,2-diamine (9.0 g, 34 mmol) was added to a flask containing 60 mL glacial acetic acid, and a solution of sodium nitrite (2.6 g, 37 mmol) dissolved in 55 mL water. The reaction mixture was stirred for 30 min at ambient temperature then cooled to 0 °C. The mixture was filtered, rinsed with water and dried under vacuum to recover 4,7-dibromo-2*H*-benzo[*d*][1,2,3]triazole (8.3 g, 30 mmol, 88%) as a beige powder. Spectroscopy was consistent with previous literature.[46]

Synthesis of 4,7-Dibromo-2-(2-octyldodecyl)-2H-benzo[*d*]-[1,2,3]triazole. 4,7-Dibromo-2*H*-benzo[*d*][1,2,3]triazole (4.7 g, 17 mmol) and potassium carbonate (4.7 g, 34 mmol) were added to a flask containing 125 mL dry, degassed *N,N*-dimethylformamide under nitrogen atmosphere. The reaction mixture was heated to 70 °C and stirred for 30 min. 9-(bromomethyl)nonadecane (6.4 g, 18 mmol) was added via syringe, and the reaction was stirred at 70 °C for 2 h. The reaction mixture was allowed to cool to ambient temperature and then quenched with 1 M HCl, and the aqueous layer was extracted with hexanes three times. The organic layer was washed three times with water, then with saturated aqueous NaCl, and dried over MgSO₄. The mixture was purified by column chromatography using 19:1 hexanes:ethyl acetate as eluent to recover 4,7-dibromo-2-(2-octyldodecyl)-2H-benzo[*d*][1,2,3]triazole (7.6 g, 14 mmol) as a pale-yellow oil. ¹H NMR (CDCl₃, 400 MHz): δ 7.43 (s, 2H), δ 4.68 (d, 2H), 2.34 (m, 1H), δ 1.23−1.33 (m, 34 H), δ 0.97−0.85 (m, 6H). ¹³C NMR (CDCl₃, 400 MHz) δ 143.7, 129.5, 110.13, 61.28, 39.1, 34.8, 32.1, 32.0, 31.7, 31.3, 29.9, 29.7, 29.7, 29.6, 29.5, 29.4, 29.3, 26.1, 25.4, 22.7, 20.8, 14.3, 11.6. HRMS-ESI: calcd, 558.18833; found, 558.20505; Δ = 2.37 ppm.

Synthesis of Acenaphthylene-(1,2-diylidene)bis-2-methoxyaniline. Formic acid (0.5 mL) was added to a flask containing

13217

dx.doi.org/10.1021/ja4073904 | *J. Am. Chem. Soc.* 2013, 135, 13212−13219

acenapthenequinone (0.99 g, 6.1 mmol), *o*-anisidine (1.66 g, 13.5 mmol), and 75 mL methanol at ambient temperature. The reaction mixture was stirred at ambient temperature for 16 h, after which it had turned dark red, and was quenched with solid potassium carbonate. The methanol was removed *in vacuo*, and the product was redissolved in methylene chloride. The organic layer was washed with water and then saturated aqueous NaCl and dried over MgSO$_4$. The mixture was concentrated and purified via column chromatography using 80:19:1 ethyl acetate:hexanes:triethylamine as eluent. Acenaphthylene-(1,2-diylidene)bis-2-methoxyaniline (0.362 mg, 0.92 mmol, 15%) was recovered as a red powder. ^{1}H NMR (CDCl$_3$, 400 MHz) δ 8.11 (t, 4H), δ 7.97 (d, 2H), δ 7.75 (dd, 2H) δ 7.43 (dd, 2H) δ 7.27−7.22 (m, 2H) δ 7.04 (d, 2H) δ 3.72 (s, 6H) ^{13}C NMR (CDCl$_3$, 400 MHz) δ 148.6, 143.3, 139.6, 132.1, 131.0, 123.9, 128.2, 126.3, 123.1, 122.1, 121.1, 119.6, 112.0, 55.8 HRMS-ESI: calcd, 393.16030; found, 393.16074; Δ = 1.10 ppm

Synthesis of Acenaphthylene-(1,2-diylidene)bis-2-methoxyaniline nickel(II) bromide (OMeAn). Under inert atmosphere, acenaphthylene-1,2-diylidene)bis-2-methoxyaniline (0.36 mg, 0.92 mmol), nickel(II) bromide ethylene glycol dimethyl ether (0.25 g, 0.83 mmol), and methylene chloride (30 mL) were stirred overnight at ambient temperature. The reaction mixture was filtered, washed with ether, and dried under suction to yield the product acenaphthylene-(1,2-diylidene)bis-2-methoxyaniline nickel(II) bromide as a green powder. ^{1}H NMR (DMSO D$_6$, 400 MHz) δ 8.41 (d (broad), 2H), δ 8.20 (dd (broad), 2H), δ 7.94 (m (broad), 2H) δ 7.61 (t (broad), 2H) δ 7.28 (dd (broad), 2H) δ 7.06 (m (broad, 2H) δ 6.93 (d, 2H), δ 3.71 (s (broad), 6H). Anal. calcd for C$_{26}$H$_{20}$O$_2$Br$_2$NNi: C, 51.03; H, 3.27. Found: C, 49.22; H 3.10.

General Procedure for Polymerization of 4,7-Dibromo-2-(2-octyldodecyl)-2H-benzo[d][1,2,3]triazole. A flame-dried Schlenk flask containing 0.1 M 4,7-dibromo-2-(2-octyldodecyl)-2H-benzo[d]-[1,2,3]triazole in dry, degassed THF was cooled to −78 °C under nitrogen atmosphere. 0.9 equiv of *n*-butyllithium was added, and the mixture stirred at −78 °C for 1 h before adding 1.0 equiv of anhydrous MgBr$_2$.(OEt$_2$). The mixture was stirred at −78 °C for 20 min, then warmed to ambient temperature, and stirred for 1 h. The reaction mixture was transferred to a flame-dried Schlenk flask containing the desired amount of catalyst and stirred at ambient temperature for 10−40 min. The polymerization was quenched with 1 mL of 5 M HCl, precipitated by the addition of methanol, and purified by washing in a Soxhlet apparatus, first with methanol and then with acetone, and then extracted with hexanes. The product, a bright-orange solid, was isolated from the hexanes fraction by concentration under vacuum. ^{1}H NMR (CDCl$_3$, 400 MHz): δ 8.90 (s, 2H), δ 4.80 (b, 2H), δ 2.47 (b, 1H), δ 1.53−1.19 (m, 32H), δ 0.80 (m, 6H). (SEC data provided in Figure 3).

General Procedure for Batch Polymerizations. A flame-dried Schlenk flask containing 0.02 M 4,7-dibromo-2-(2-octyldodecyl)-2H-benzo[d][1,2,3]triazole and 0.004 M docosane in dry, degassed THF was cooled to −78 °C under nitrogen atmosphere. 0.9 equiv of *n*-butyllithium was added, and the mixture stirred at −78 °C for 1 h before adding 1.0 equiv of anhydrous MgBr$_2$.(OEt$_2$). The mixture was stirred at −78 °C for 20 min, then warmed to ambient temperature, and stirred for 1 h. The reaction mixture was then cooled to 0 °C, and the catalyst was added as a suspension in dichloromethane via syringe. Aliquots were removed and quenched with 5 M aqueous HCl, neutralized with sodium bicarbonate, and extracted with dichloromethane. Each aliquot was analyzed using gas chromatography, and the monomer consumption was determined relative to the docosane internal standard. Molecular weight and polydispersity were determined on the polymer sample without Soxhlet extraction. (SEC data provided in Table 1).

Chain Extension Polymerization. A flame-dried Schlenk flask containing 0.342 g (0.61 mmol) 4,7-dibromo-2-(2-octyldodecyl)-2H-benzo[d][1,2,3]triazole in 6.0 mL dry, degassed THF was cooled to −78 °C under nitrogen atmosphere. 0.58 mmol of *n*-butyllithium was added, and the mixture stirred at −78 °C for 1 h before adding 0.165 g (0.61 mmol) of anhydrous MgBr$_2$.(OEt$_2$). The mixture was stirred at −78 °C for 20 min, then warmed to ambient temperature, and stirred

for 1 h. 3.0 mL of the reaction mixture was transferred to a flame-dried Schlenk flask containing 7.1 mg (0.012 mmol, 4 mol %) of the OMeAn catalyst and stirred at ambient temperature for 15 min. 0.5 mL of the reaction mixture was removed and quenched with 5 M aqueous HCl. The remaining 3.0 mL of the activated monomer mixture was then added to the polymerization flask and stirred at ambient temperature for 40 min. The polymerization was then quenched with 5 M aqueous HCl. Each polymer fraction was then precipitated in methanol, washed with acetone, and extracted with hexanes prior to SEC analysis (results shown in Figure 6).

Catalyst DFT Calculations. Calculations were carried out using the B3LYP hybrid functional in Gaussian 09.[54−56] Geometries were initially optimized using a split basis set consisting of 6-31G(d)[56,57] for carbon, hydrogen, nitrogen, oxygen, and fluorine, LANL2DZ[58,59] for nickel, and Ahlrichs SVP[60,61] for bromine. These geometries were then used as a starting point for the single point energy calculations used to construct the reaction coordinate consisting of a split basis set: 6-311+G(d,p)[62,63] for carbon, hydrogen, nitrogen, oxygen, and fluorine, SDD[64] for nickel, and TZVP[65,66] for bromine.

Polymer DFT Calculations. Calculations were carried out using the B3LYP hybrid functional in Gaussian 09. Energy levels of the polymer were determined using a 6-31G(d) basis set for both geometry optimization and energy levels.[67] Alkyl chains were replaced with methyl groups to reduce the computation time.

■ ASSOCIATED CONTENT

Ⓢ Supporting Information

^{1}H NMR of the metathesis quenching experiments. Polymerization procedure, kinetics, and molecular weight data using Ni(dppe)Cl$_2$. ^{1}H NMR, electrochemistry, and thin-film optical absorption of PBTz. Representative SEC traces for polymers resulting from each catalyst. Thin-film fluorescence quenching of P3HT:PBTz films. Cartesian coordinates and energy levels of the calculated stationary points for the catalyst−monomer complexes and octomers of P3AT and PBTz. Complete ref 56. This material is available free of charge via the Internet at http://pubs.acs.org.

■ AUTHOR INFORMATION

Corresponding Author
dseferos@chem.utoronto.ca

Notes
The authors declare no competing financial interest.

■ ACKNOWLEDGMENTS

■ REFERENCES

(1) Britovsek, G. J.; Gibson, V. C.; Wass, D. F. *Angew. Chem., Int. Ed.* **1999**, *38*, 428−447.

(2) Fürstner, A. *Angew. Chem., Int. Ed. Engl.* **2000**, *39*, 3012−3043.

(3) Kaminsky, W. *J. Polym. Sci., Part A: Polym. Chem.* **2004**, *42*, 3911−3921.

(4) Astruc, D. *New J. Chem.* **2005**, *29*, 42−56.

(5) McCullough, R. D.; Lowe, R. D. *J. Chem. Soc., Chem. Commun.* **1992**, 70−72.

(6) Chen, T. A.; Wu, X.; Rieke, R. D. *J. Am. Chem. Soc.* **1995**, *117*, 233−244.

(7) Loewe, R. S.; Ewbank, P. C.; Liu, J.; Zhai, L.; McCullough, R. D. *Macromolecules* **2001**, *34*, 4324−4333.

(8) Roncali, J. *Chem. Rev.* **1992**, *92*, 711−738.

(9) Yokoyama, A.; Miyakoshi, R.; Yokozawa, T. *Macromolecules* **2004**, *37*, 1169−1171.

(10) Sheina, E. E.; Liu, J.; Iovu, M. C.; Laird, D. W.; McCullough, R. D. *Macromolecules* **2004**, *37*, 3526−3528.

(11) Iovu, M. C.; Sheina, E. E.; Gil, R. R.; McCullough, R. D. *Macromolecules* **2005**, *38*, 8649−8656.

(12) Beryozkina, T.; Senkovskyy, V.; Kaul, E.; Kiriy, A. *Macromolecules* **2008**, *41*, 7817−7823.

(13) Tkachov, R.; Senkovskyy, V.; Komber, H.; Sommer, J.-U.; Kiriy, A. *J. Am. Chem. Soc.* **2010**, *132*, 7803−7810.

(14) Kiriy, A.; Senkovskyy, V.; Sommer, M. *Macromol. Rapid Commun.* **2011**, *32*, 1503−1517.

(15) Bryan, Z. J.; McNeil, A. J. *Chem. Sci.* **2013**, *4*, 1620−1624.

(16) Zenkina, O. V.; Karton, A.; Freeman, D.; Shimon, L. J. W.; Martin, J. M. L.; van der Boom, M. E. *Inorg. Chem.* **2008**, *47*, 5114−5121.

(17) Hollinger, J.; Jahnke, A. A.; Coombs, N.; Seferos, D. S. *J. Am. Chem. Soc.* **2010**, *132*, 8546−8547.

(18) Jahnke, A. A.; Djukic, B.; McCormick, T. M.; Buchaca Domingo, E.; Hellmann, C.; Lee, Y.; Seferos, D. S. *J. Am. Chem. Soc.* **2013**, *135*, 951−954.

(19) Traina, C. A.; Bakus, R. C., II; Bazan, G. C. *J. Am. Chem. Soc.* **2011**, *133*, 12600−12607.

(20) Bryan, Z. J.; Smith, M. L.; McNeil, A. J. *Macromol. Rapid Commun.* **2012**, *33*, 842−847.

(21) Nanashima, Y.; Yokoyama, A.; Yokozawa, T. *Macromolecules* **2012**, *45*, 2609−2613.

(22) Ono, R. J.; Kang, S.; Bielawski, C. W. *Macromolecules* **2012**, *45*, 2321−2326.

(23) Kozycz, L. M.; Gao, D.; Hollinger, J.; Seferos, D. S. *Macromolecules* **2012**, *45*, 5823−5832.

(24) Palermo, E. F.; McNeil, A. J. *Macromolecules* **2012**, *45*, 5948−5955.

(25) Hollinger, J.; Sun, J.; Gao, D.; Karl, D.; Seferos, D. S. *Macromol. Rapid Commun.* **2013**, *34*, 437−441.

(26) Kline, R. J.; McGehee, M. D.; Kadnikova, E. N.; Liu, J.; Fréchet, J. M. J.; Toney, M. F. *Macromolecules* **2005**, *38*, 3312−3319.

(27) Kozycz, L. M.; Gao, D.; Seferos, D. S. *Macromolecules* **2013**, *46*, 613−621.

(28) Li, L.; Hollinger, J.; Jahnke, A. A.; Petrov, S.; Seferos, D. S. *Chem. Sci.* **2011**, *2*, 2306−2310.

(29) Coffin, R. C.; Peet, J.; Rogers, J.; Bazan, G. C. *Nat. Chem.* **2009**, *1*, 657−661.

(30) Tsoi, W. C.; James, D. T.; Domingo, E. B.; Kim, J. S.; Al-Hashimi, M.; Murphy, C. E.; Stingelin, N.; Heeney, M.; Kim, J.-S. *ACS Nano* **2012**, *6*, 9646−9656.

(31) Zen, A.; Pflaum, J.; Hirschmann, S.; Zhuang, W.; Jaiser, F.; Asawapirom, U.; Rabe, J. P.; Scherf, U.; Neher, D. *Adv. Funct. Mater.* **2004**, *14*, 757−764.

(32) Elmalem, E.; Kiriy, A.; Huck, W. T. S. *Macromolecules* **2011**, *44*, 9057−9061.

(33) Nanashima, Y.; Shibata, R.; Miyakoshi, R.; Yokoyama, A.; Yokozawa, T. *J. Polym. Sci. A Polym. Chem.* **2012**, *50*, 3628−3640.

(34) Hwang, Y.-J.; Ren, G.; Murari, N. M.; Jenekhe, S. A. *Macromolecules* **2012**, *45*, 9056−9062.

(35) Usta, H.; Risko, C.; Wang, Z.; Huang, H.; Deliomeroglu, M. K.; Zhukhovitskiy, A.; Facchetti, A.; Marks, T. J. *J. Am. Chem. Soc.* **2009**, *131*, 5586−5608.

(36) Letizia, J. A.; Salata, M. R.; Tribout, C. M.; Facchetti, A.; Ratner, M. A.; Marks, T. J. *J. Am. Chem. Soc.* **2008**, *130*, 9679−9694.

(37) Babel, A.; Jenekhe, S. A. *J. Am. Chem. Soc.* **2003**, *125*, 13656−13657.

(38) Yokozawa, T.; Nanashima, Y. *ACS Macro Lett.* **2012**, *1*, 862−866.

(39) Nicolai, H. T.; Kuik, M.; Wetzelaer, G. A. H.; de Boer, B.; Campbell, C.; Risko, C.; Bredas, J. L.; Blom, P. W. M. *Nat. Mater.* **2012**, *11*, 882−887.

(40) Senkovskyy, V.; Tkachov, R.; Komber, H.; John, A.; Sommer, J.-U.; Kiriy, A. *Macromolecules* **2012**, *45*, 7770−7777.

(41) Senkovskyy, V.; Tkachov, R.; Komber, H.; Sommer, M.; Heuken, M.; Voit, B.; Huck, W. T. S.; Kataev, V.; Petr, A.; Kiriy, A. *J. Am. Chem. Soc.* **2011**, *133*, 19966−19970.

(42) Lee, S. R.; Bryan, Z. J.; Wagner, A. M.; McNeil, A. J. *Chem. Sci.* **2012**, *3*, 1562−1566.

(43) Lanni, E. L.; McNeil, A. J. *Macromolecules* **2010**, *43*, 8039−8044.

(44) Lee, S. R.; Bloom, J. W. G.; Wheeler, S. E.; McNeil, A. J. *Dalton Trans.* **2013**, *42*, 4218−4222.

(45) Yang, R.; Tian, R.; Yan, J.; Zhang, Y.; Yang, J.; Hou, Q.; Yang, W.; Zhang, C.; Cao, Y. *Macromolecules* **2005**, *38*, 244−253.

(46) Tanimoto, A.; Yamamoto, T. *Adv. Synth. Catal.* **2004**, *346*, 1818−1823.

(47) Johnson, L. K.; Killian, C. M.; Brookhart, M. *J. Am. Chem. Soc.* **1995**, *117*, 6414−6415.

(48) Killian, C. M.; Tempel, D. J.; Johnson, L. K.; Brookhart, M. *J. Am. Chem. Soc.* **1996**, *118*, 11664−11665.

(49) Gates, D. P.; Svejda, S. A.; Oñate, E.; Killian, C. M.; Johnson, L. K.; White, P. S.; Brookhart, M. *Macromolecules* **2000**, *33*, 2320−2334.

(50) Ouhib, F.; Desbief, S.; Lazzaroni, R.; De Winter, J.; Gerbaux, P.; Jérôme, C.; Detrembleur, C. *Macromolecules* **2012**, *45*, 6796−6806.

(51) Magurudeniya, H. D.; Sista, P.; Westbrook, J. K.; Ourso, T. E.; Nguyen, K.; Maher, M. C.; Alemseghed, M. G.; Biewer, M. C.; Stefan, M. C. *Macromol. Rapid Commun.* **2011**, *32*, 1748−1752.

(52) Sheina, E. E.; Iovu, M. C.; McCullough, R. D. *Polym. Prepr. (Am. Chem. Soc., Div. Polym. Chem.)* **2005**, *46* (2), 1070−1071.

(53) Yoshikai, N.; Matsuda, H.; Nakamura, E. *J. Am. Chem. Soc.* **2008**, *130*, 15258−15259.

(54) Becke, A. D. *J. Phys. Chem.* **1993**, *98*, 5648−5652.

(55) Becke, A. D. *J. Phys. Chem.* **1996**, *104*, 1040−1047.

(56) Frisch, M. J. et al. *Gaussian 09*; Gaussian, Inc.: Wallingford, CT, 2009.

(57) Petersson, G. A.; Bennett, A.; Tensfeldt, T. G.; Al-Laham, M. A.; Shirley, W. A.; Mantzaris, J. *J. Chem. Phys.* **1988**, *89*, 2193−2218.

(58) Petersson, G. A.; Al-Laham, M. A. *J. Chem. Phys.* **1991**, *94*, 6081−6090.

(59) Hay, P. J.; Wadt, W. R. *J. Chem. Phys.* **1985**, *82*, 284−298.

(60) Hay, P. J.; Wadt, W. R. *J. Chem. Phys.* **1985**, *82*, 270−283.

(61) Hay, P. J.; Wadt, W. R. *J. Chem. Phys.* **1985**, *82*, 299−310.

(62) Schaefer, A.; Huber, C.; Ahlrichs, R. *J. Chem. Phys.* **1992**, *97*, 2571−2577.

(63) Schaefer, A.; Huber, C.; Ahlrichs, R. *J. Chem. Phys.* **1994**, *100*, 5829−5835.

(64) McLean, A. D.; Chandler, G. S. *J. Chem. Phys.* **1980**, *72*, 5639−48.

(65) Raghavachari, K.; Binkley, J. S.; Seeger, R.; Pople, J. A. *J. Chem. Phys.* **1980**, *72*, 650−654.

(66) Dolg, M.; Wedig, U.; Stoll, H.; Preuss, H. *J. Chem. Phys.* **1987**, *86*, 866−872.

(67) McCormick, T. M.; Bridges, C. R.; Carrera, E. I.; DiCarmine, P. M.; Gibson, G. L.; Hollinger, J.; Kozycz, L. M.; Seferos, D. S. *Macromolecules* **2013**, *46*, 3879−3886.

(68) Ellinger, S.; Ziener, U.; Thewalt, U.; Landfester, K.; Möller, M. *Chem. Mater.* **2007**, *19*, 1070−1075.